Comparative performance evaluations of nanomaterials mixed polysulfone: A scale-up approach through…

Article *in* Desalination · September 2017

DOI: 10.1016/j.desal.2017.08.020

5 authors, including:

Abdel-Hameed Mostafa El-Aassar
Egyptian Desalination Research Center of Exc…
15 PUBLICATIONS **29** CITATIONS
SEE PROFILE

Rasel Das
Leibniz Institute of Surface Modification
28 PUBLICATIONS **308** CITATIONS
SEE PROFILE

Desalination xxx (xxxx) xxx–xxx

Contents lists available at ScienceDirect

Desalination

journal homepage: www.elsevier.com/locate/desal

Comparative performance evaluations of nanomaterials mixed polysulfone: A scale-up approach through vacuum enhanced direct contact membrane distillation for water desalination

Mohamed S. Fahmey[a], Abdel-Hameed Mostafa El-Aassar[a,*], Mustafa M.Abo-Elfadel[a], Adel Sayed Orabi[b], Rasel Das[c,*]

[a] Egyptian Desalination Research Center of Excellence (EDRC), Desert Research Center, El-Matariya, P.O.B 11753, Cairo, Egypt
[b] Chemistry Department, Faculty of Science, Suez Canal University-41522, Ismailia, Egypt
[c] Chemical Department, Leibniz Institute of Surface Modification, Permoserstr 15, D-04318 Leipzig, Germany

ARTICLE INFO

Keywords:
Polysulfone
Nanocomposite
Membrane distillation
Water desalination

ABSTRACT

Doping of multi-walled carbon nanotube (MWCNT), silicon dioxide (SiO_2), titanium dioxide (TiO_2) and zinc oxide (ZnO) into polysulfone (PSf) flat sheet membranes was prepared by phase inversion process. The characterizations of the PSf and PSf-MWCNT, PSf-SiO_2, PSf-TiO_2 and PSf-ZnO membranes were achieved using Fourier transform infrared spectroscope, contact angle measurement, dynamic mechanical analyzer, thermogravimetric analysis and scanning electron microscope. Vacuum enhanced direct contact membrane distillation unit was used for evaluating the efficacy of prepared membranes in water desalination. Optimizing the operational procedures and water characteristics ensured a high slat rejection of 99.99% using the prepared membranes. The highest permeate flux obtained in the order of MWCNT (41.58) > SiO_2 (38.84) > TiO_2(35.6) > ZnO (34.42 $L/m^2 \cdot h$) with optimized concentration of 1.0, 0.5, 0.75, 0.5 wt% relative to PSf weight, i.e. 15%. The optimum operational conditions included feed and permeate temperatures 60 °C and 20 °C, respectively, synthetic NaCl feed water with salinity was 10,000 ppm.

1. Introduction

Clean water is very essential for all aspects of human life, and in some regions can be difficult to obtain it from wells or rivers. In these situations, some water resources including brackish water and sea water could act as abundant sources for purification [1]. With the advent of rapid industrialization, cultivation, and growing population; the water became unsuitable to drink. Even though attempts have been made for full utilization of the available natural water resources, it has become necessary to adopt different desalination techniques to convert saline water resources into good water quality [2].

Membrane distillation (MD) is a process that applied differences in vapor pressure to permeate water vapor through the hydrophobic porous membrane and rejects non-volatile component present in the water [3]. MD is popular for water desalination due to many advantages: a) lower operating temperatures than that of traditional distillation process, b) lower operating hydrostatic pressures, c) high rejection factors i.e. 100% (theoretical) when solutions containing nonvolatile solutes, d) less demanding membrane's mechanical properties, and e) membrane fouling in MD is a less frequent problem as compared with the pressure driven processes, e.g. reverse osmosis (RO). Direct contact (DC) MD is the simplest MD configuration and is widely employed in the water desalination. In DCMD, the hot feed solution is in direct contact with the hot membrane side surface. Therefore, evaporation takes place at the feed membrane surface. The vapor is moved by the pressure difference across the membrane to the permeate side and condenses inside the membrane module [3]. The performance of DCMD can be improved by different ways. One of them is vacuum-enhanced direct contact membrane distillation (VEDCMD) in which the cooler water stream flows under negative pressure (vacuum) [4]. VEDCMD has been shown to increase the permeate flux up to 85% compared to the conventional DCMD configuration [5].

Recently, a considerable attention has been paid to the preparation of nanocomposite membrane for water desalination due to its improved productivities including high water permeability with salts rejection [6,7]. Although a remarkable development has been noticed in using nanocomposite for filtration-based desalination systems [8], a few reports are available to test such membranes in MD system [9]. To our

* Corresponding authors.
E-mail addresses: amelaassar@edrc.gov.eg (A.-H.M. El-Aassar), raseldas@daad-alumni.de (R. Das).

http://dx.doi.org/10.1016/j.desal.2017.08.020
Received 17 May 2017; Received in revised form 14 August 2017; Accepted 25 August 2017

knowledge, there is no report published on polysulfone (PSf) based nanocomposite membrane where a comparative study has been taken not only to dope carbon-based nanomaterial like multi-walled carbon nanotube (MWCNT), but also nanoparticles including silicon dioxide (SiO_2), titanium dioxide (TiO_2), and zinc oxide (ZnO) in VEDCMD process. Testing this hypothesis is important, since it has been observed that the significant improvement of productivities of polymer (e.g. polypropylene) membranes using MWCNT in VEDCMD process [10].

In this work, preparation and modification of PSf flat sheet membranes using different nanomaterials such as MWCNT, SiO_2, TiO_2, and ZnO were achieved. The prepared membranes were characterized using Fourier transform infrared (FTIR) spectroscope, contact angle measurement, dynamic mechanical analyzer (DMA), thermo-gravimetric analysis (TGA) and scanning electron microscope (SEM). The performance of the prepared membranes in water desalination via VEDCMD technique was evaluated through studying the influence of membrane preparation conditions, feed water characteristics and operating conditions.

2. Experimental

2.1. Materials

PSf (Udel-3500), *N*, *N*-dimethylacetamide (DMAc), *N*, *N*-dimethylformamide (DMF) were supplied by Fisher Chemical. MWCNT with outer diameter of 10–15 nm, inner diameter of 2–6 nm and length of 0.1–10 μm, TiO_2 anatase nano-powder having < 25 nm particles size, ZnO nano-powder having < 100 nm particle size, SiO_2 nano-particles having 200 nm particle size were supplied by Sigma Aldrich. The other chemicals such as the chemical additive, inorganic salt as LiCl, and feed salt such as; sodium sulfate (Na_2SO_4), sodium chloride (NaCl) and magnesium sulfate ($MgSO_4$) were supplied by Adowic Co.

2.2. Preparation of neat and nanomaterials modified hydrophobic polysulfone membrane

For neat PSf membranes, the casting solution was prepared by dissolving a specific weight 3.0 g of PSf into 20 mL of DMF. The solution was gently heated at 100 °C with continued stirring until complete dissolution occurred. It was then degased for enough time at room temperature. Secondly, prior to preparing PSf/MWCNT, we measured 0.05–0.3 g of MWCNT correspond to 0.25–1.5 wt% and mixed into 20 mL of PSf containing DMF. Similarly PSf/SiO_2 (0.25–1 wt%), PSf/TiO_2 (0.25–1 wt%) and PSf/ZnO (0.25–1 wt%) were prepared by measuring 0.05–0.2 g of SiO_2, TiO_2 and ZnO into 20 mL of PSf containing DMF. After that, the PSf/MWCNT, PSf/SiO_2, PSf/TiO_2 and PSf/ZnO mixture solutions were casted on a glass plate using the film applicator. The glass plate was immersed in the coagulation bath immediately to obtain the flat sheet membrane. The thicknesses of these membranes were adjusted at 200 μm. Finally, all the membranes were washed in de-ionized water, dried completely and kept in a dry place until characterization and performance processes were taken.

2.3. Characterization of the membranes

The swelling, conversion and gelation values were obtained using following measurements. The clean and dried membranes of known weights (W_o) were immersed in distilled water at 25 °C until equilibrium has been reached (after 24 h). The membranes were removed, plotted by filtrate paper and quickly weighted (W_w) then let them to dry again in room temperature for 24 h and weighted again (W_d). The swelling (%) was calculated as Eq. (1):

$$\text{Swelling}\% = \frac{W_w - W_d}{W_d} \times 100 \quad (1)$$

where W_d and W_w represent the weights of the dry and wet membranes, respectively. Also, the conversion (%) was calculated as Eq. (2):

$$\text{Conversion}\% = \frac{W_d}{W_o} \times 100 \quad (2)$$

where W_d and W_o represent the weights of the dry and initial membranes, respectively.

The dry membrane was immersed in hot water at 60 °C for 24 h. The membranes were removed from hot water, plotted by filtrate paper and quickly weighed W_h then let it to dry again in room temperature for 24 h and weighted again (W_{dh}).The gelation percent was calculated as Eq. (3):

$$\text{Gelation}\% = \frac{W_{dh}}{W_o} \times 100 \quad (3)$$

FTIR analysis of the prepared membranes was carried out using Bruker Vertex70 FT-IR spectrometer model. The contact angle of water on prepared membranes was determined at room temperature using the sessile droplet method on a Drop Shape Analyzer-DSA25. At least five angles were measured for each sample, and then the average value was calculated and reported. Mechanical measurements were carried out through measuring both tensile strength young modules and elongation percent by using DMA apparatus (Module DMA Q800 V21.1 Build 51-Controlled Force). The TGA of prepared membranes was carried out by using a Shimadzu TGA system of type TGA-50H using N_2 with flow rate 20 mL/min and temperature rate holder 10 °C/min sample weight varied in rang (1–2 mg). The surface morphology of the membranes was studied using SEM Model Quanta FEG250 SEM (FEI Company).

2.4. Feed water preparation

NaCl synthetic feed solutions were used with different salinities ranged from 2000 to 50,000 ppm. Other two different salt types (Na_2SO_4, and $MgSO_4$) were used as feed solutions with concentrations ranged from 2000 to 5000 ppm.

2.5. The VEDCMD experimental setup

The VEDCMD experimental setup is schematically depicted in Fig. 1. The membrane module consisted of two compartments: the feed side and the permeate side where (T_f) and (T_p) represent feed and permeate temperature, respectively: and (P_f) and (P_p) represent feed and permeate pressure, respectively. The compartments were made of polyacrylic to resist the corrosion by feed solutions. The module positioned horizontally so that the feed solution flowed through the bottom compartment of the module while the cooling water passed through the upper compartment. The feed and permeate separated by a membrane with effective area of 0.0019 m^2. The cooler (Chiller NESLAB CFT-75 Refrigerated Re-circulator, USA) was used for regulating the cold stream. On the other hand, thermostatic hot feed water bath was used for controlling the hot stream. Two flow meters (Blue-White F-550

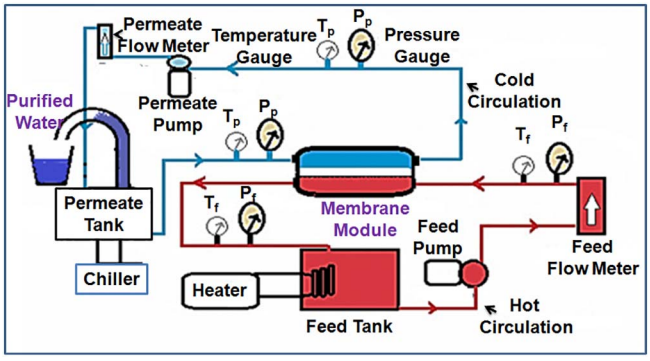

Fig. 1. Diagram of VEDCMD experimental unit used in this study.

model, USA) and (Green-life Drinking Water System, USA) were used with ranges 1–7 L/min and 5–35 L/min for permeate feed circulations, respectively. Two centrifugal pumps and two pressure gauges (WSG-SOLO model 100 mm radial) with pressure range from (− 30 to 70 psi) were used. Also four thermocouples (accuracy ± 0.1 °C) were used for evaluating the temperatures of both streams. The tanks of 15 and 4.8 L were used for hot and cold streams, respectively. The feed and cold solutions were contained in double-walled reservoirs and circulated through the membrane module using centrifugal pumps.

All obtained data from the prepared membranes with stable flux were reported as mean value of the measured flux every hour over a 4–6 h period. The purity of the water extracted was determined through water conductivity using an electrical conductivity meter (EC470-L, ISTEK, Korea). It should be noted here that any increase in permeate conductivity indicated that liquid water passes through the membrane so that result is rejected, in other words, the salt rejection of all membranes was 99.99%. In order to check the presence of leakages in the system, as well as the membrane hydrophobicity, the volume in the graduated cylinder was observed when only the hot stream was re-calculated for at least 30 min before starting the experiment. Each experiment was then initiated only when no variation was reported on the display for the time of observation. During the experiments, the feed was at (0.5 bar) and its flow rate was varied between 6 and 15 L/min, while the feed temperature was varied between 40 and 60 °C. In VEDCMD tests, the distillate flow rate was kept at about 2.7 L/min with negative pressure (− 3) psi and the distillate temperature was in the range of 20 °C [10].

3. Results and discussion

3.1. Characterization of membranes

3.1.1. Swelling, conversion and gelation measurements

Swelling, conversion and gelation of the neat PSf and the modified PSf membranes are shown in Fig. 2. It shows different behaviors of the membranes according to the nanomaterial types. In general, the swelling (%) of PSf was increased upon mixing with nanomaterials as compared with that of the neat PSf membrane. The swelling (%) follows the trend of PSf/SiO_2 > PSf/TiO_2 > PSf/MWCNT > PSf/ZnO (Fig. 2). The highest swelling of SiO_2 was due to its larger particle size (200 nm) used in this study which might create macrovoids in membrane sublayers as compared with other nanomaterials used. These voids might act as water uptake home and also formation of pores in surface, i.e., the porosity of membranes that allow the water penetration into the PSf [11]. On the other hand, the conversion and gelation (%) were high for all prepared membranes. The conversion (%) of all membranes was ranged from 93.62 to 95.56, while the gelation (%) was between 93.62 and 95.56 (Fig. 2).

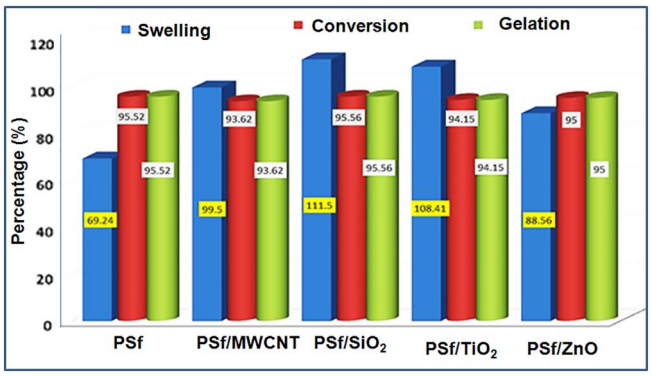

Fig. 2. Swelling, conversion and gelation percentages of neat and modified PSf membranes.

Table 1
Contact angles of neat (M1) and modified (M2–M9) PSf membranes.

Membrane code	Nanomaterials (%)	Contact angle	Contact Angle reinforcement
M1	–	77 ± 2	–
M2	MWCNT (1)	82 ± 3	5 ± 3
M3	MWCNT (0.75)	80 ± 3	3 ± 3
M4	SiO_2 (0.5)	74 ± 2	− 3 ± 2
M5	SiO_2 (0.75)	69 ± 2	− 8 ± 2
M6	TiO_2 (0.5)	73 ± 2	− 4 ± 2
M7	TiO_2 (0.75)	71 ± 2	− 6 ± 2
M8	ZnO (0.5)	70 ± 2	− 7 ± 2
M9	ZnO (0.75)	69 ± 2	− 1 ± 2

3.1.2. FTIR analysis

The FTIR spectra of the neat and the modified PSf membranes are shown in Supplementary File Fig. S1. It is obvious that all prepared membranes contained very similar functional groups due to the appearance of similar peaks. This is due to the chemical compositions of the membranes. The absorption bands of the material corresponds to the PSf groups, being in good agreement with standard PSf at 1044 cm^{-1} (SO_3H), 1106 cm^{-1} (C—O), 1150 cm^{-1} (R-SO_2-R), 1241 cm^{-1} (C—O), 1488 cm^{-1} (aromatic bond), 2966 cm^{-1} (aliphatic CH), 2879 cm^{-1} (aromatic CH) and 3362 cm^{-1} (OH) [12]. The embedded nanomaterials have different oxy-functional groups which might be overlap with real PSf membranes. Absence of their unique bands in this work could also due to using small concentration used which might be encapsulated under PSf polymeric chains [13,14].

3.1.3. Contact angle analysis

Determination of contact angle is very important for membrane distillation. The contact angles of the PSf (15 wt%) and best eight modified membranes having different concentrations of nanomaterials are revealed in Table 1. As it is clearly postulated from Table 1 that there is a reinforcement of the contact angle value for PSf upon mixing with pristine hydrophobic MWCNT [10]. On the contrary, the addition of SiO_2, TiO_2 and ZnO reduced the contact angle of PSf. This was due to oxide forms of these nanoparticles that might act as active materials on the PSf membrane surface and form hydrogen bonds with water [15]. The higher contact angles were sponsored by using MWCNT (0.75–1) > SiO_2(0.5) > TiO_2(0.5–0.75) > ZnO(0.5 wt%).

3.1.4. Mechanical properties analysis

The mechanical properties of the selected membranes are listed in Supplementary Table S1. These properties include young modulus, tensile strength, and elongation at break of the membranes. According to Table S1, it is clear that there is a decrement in tensile strength for all modified PSf membranes with respect to the neat PSf membrane. The Young modulus decreased for modified membranes with the different nanomaterials except TiO_2 (0.75 wt%) and ZnO (0.5–0.75 wt%). This decrement is due to the nanoparticles nature and its concentration [16]. It is important to mention that there is a slightly improved in both Young modulus and tensile strength at high concentrations for all nanomaterials except MWCNT. Wu et al. [17] suggested that the mechanical properties of organic polymer membranes generally improve with the increasing nanomaterials due to “cross-linking effects” to bear the stress of the membrane load. But further increasing the concentration of nanomaterials could aggregate themselves and subsequently reduces the mechanical properties, and causes the formation of macrovoids and microvoids in subsurface layer. These lead to the formation of more fragile membranes.

3.1.5. Thermo-gravimetric analysis

The TGA and differential TGA plots of neat PSf and the modified membranes are shown in Supplementary File (Fig. S2). It is obvious that

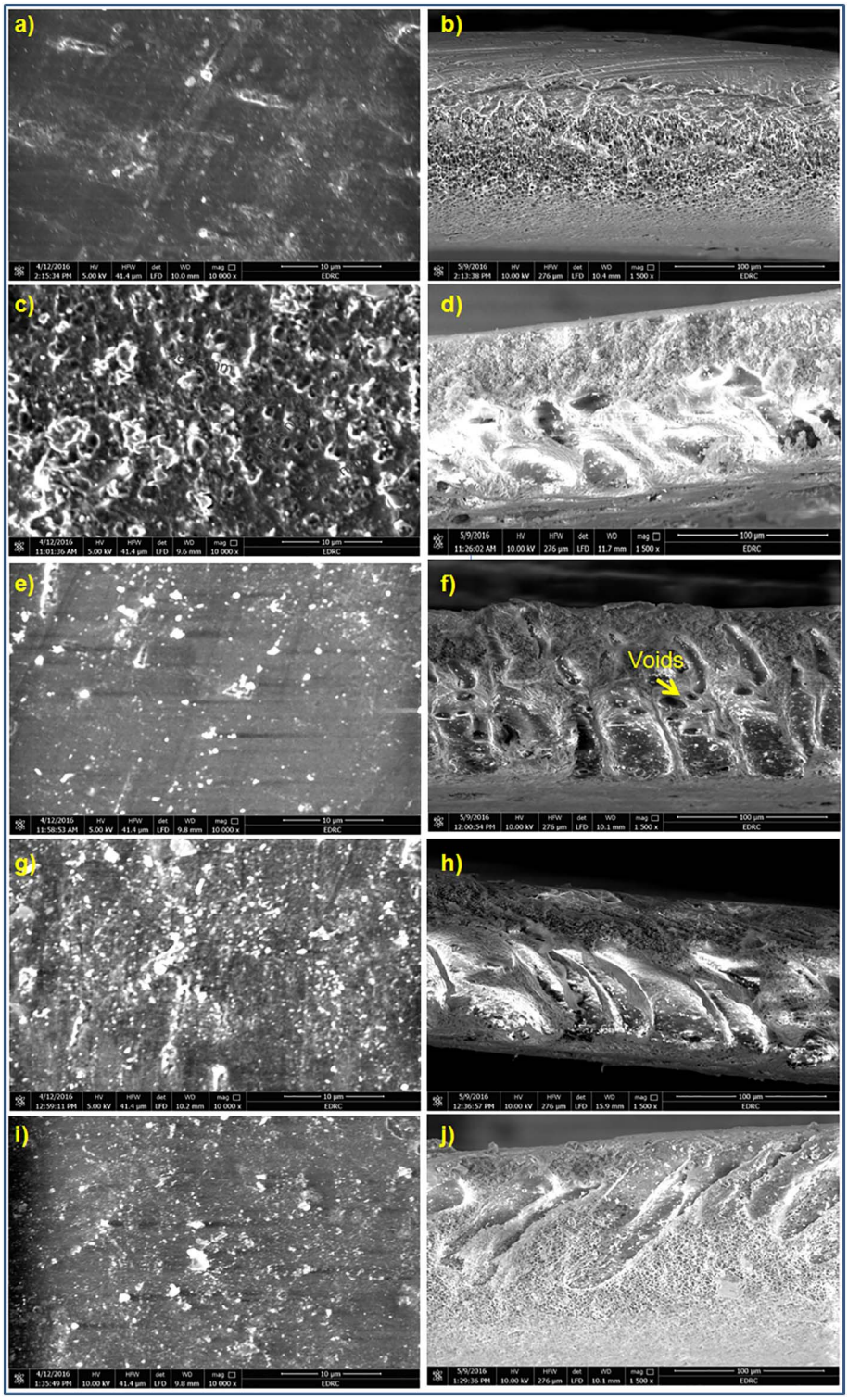

Fig. 3. SEM images of surfaces (left panel) and cross-sections (right panel) of neat PSf (a and b), PSf/MWCNT (c and d), PSf/SiO_2 (e and f), PSf/TiO_2 (g and h) and PSf/ZnO (i and j).

all the membranes showed a slow decrement in the range from 100 °C to 500 °C before the steep slope. This behavior was contributed by both the elimination of moisture trapped inside the membranes and the thermal stability of polymeric material [18]. At temperature above 500 °C, the membranes showed a greater decrement in weight percentage with the increasing temperature due to their decomposition. This decomposition occurred through two steps; the first step started in temperature ranged from 500 °C to 580 °C. The second step started from 585 °C to 760 °C. The TGA curves showed that PSf/MWCNTs membrane was the most stable membrane as compared with the other membranes.

3.1.6. Scanning electron microscope analysis

SEM images of the PSf (a and b) and modified membranes (c–j) at a scale of 100 μm are shown in Fig. 3. It can be seen that all membranes exhibit an asymmetric structure with a thick skin layer. However, it is clear that the type of nanomaterial significantly affected the morphology of the membrane (Fig. 3(c–j)). For the neat PSf membrane, the structure is reasonably spongy in nature (Fig. 3(b)). Most of the modified membranes appeared more voids like tubes and reduced from spongy structure (Fig. 3(c–j)). The number of voids could explain the swelling behavior of the modified membranes as shown in Fig. 2.

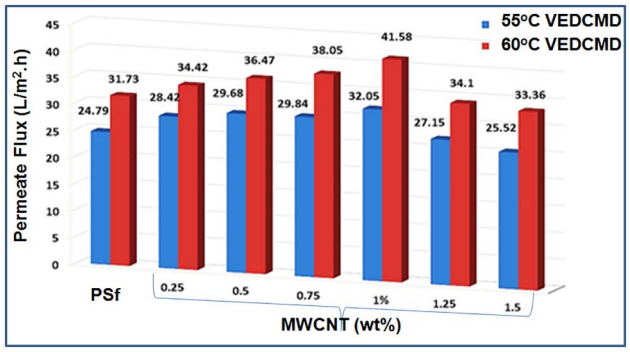

Fig. 4. Effect of MWCNT concentrations on PSf membrane performance.

3.2. Performance optimizations of modified PSf membranes

We first optimized all the parameters including operational settings, and features of neat PSf membranes as discussed in details in Supplementary File (Sections S1.1 and 1.2). Then we maximized the performances of PSf membranes, especially in terms of increasing permeate flux using different concentrations of MWCNT, SiO_2, TiO_2 and ZnO at optimized conditions. Firstly, we used MWCNT as tubular nano-filler [6] for doping into PSf using DMF solvent. DMF was used due to selected optimal solvent for PSf, as well as a suitable dispersion medium for MWCNTs as reported in the previous works [19,20]. Different membranes of PSf doped with MWCNTs were prepared using different MWCNT concentrations ranged from 0.25 to 1.5 wt% related to PSf weight, i.e. 15 (wt%). All prepared PSf/MWCNT membranes were evaluated in VEDCMD at two different feed temperatures as shown in Fig. 4. It can be seen that all modified membranes showed a significant increase in the permeate flux as compared with that of the neat PSf membrane. The increasing of permeate flux was proportionally linear with increasing MWCNT concentrations. This increase of the permeate flux was due to increasing the porosity and the surface hydrophobicity of PSf-MWCNT membranes [21]. However, permeate flux declined by further increasing of MWCNT concentrations (i.e. > 1 wt%)). This might be due to a denser membrane structure is formed which could increase the viscosity of the casting solution that led to smaller pore size as well as aggregation of MWCNT and its impurities [20,22].

Secondly, different PSf/SiO_2 membranes were prepared using different SiO_2 concentrations ranged from 0.25 to 1 wt% as shown in Fig. 5. It is clear that the increase of permeate flux is possible by increasing SiO_2 concentration up to 0.5 wt%. It might be due to the formation of void space like tubes (Fig. 3) which support the mass transfer process. On the other hand, further increasing of SiO_2; i.e. at 0.75 wt%, a deterioration in the permeate flux was observed. This phenomenon was due to the effect of hydrophilicity of SiO_2 that start to appear, so pores wetting and pores blocking took place. Similar effect has been noticed for 1 wt% of SiO_2.

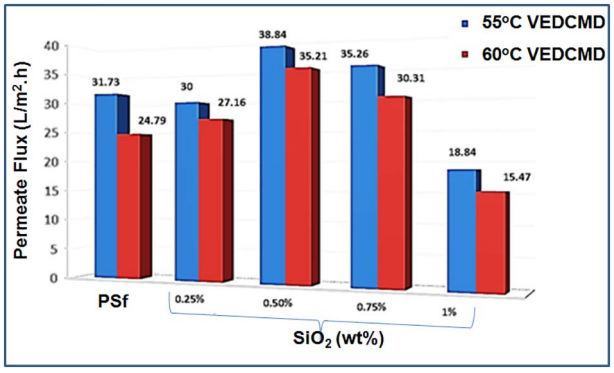

Fig. 5. Effect of SiO_2 concentration on PSf membrane performance.

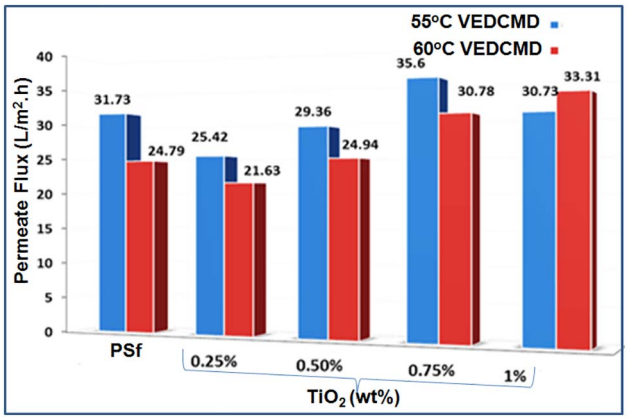

Fig. 6. Effect of TiO_2 concentration on PSf membrane performance.

Thirdly, TiO_2 was used as a pore former nano-filler at different concentrations ranged from 0.25 to 1 wt% as shown in Fig. 6. It is obvious that by using 0.25 and 0.5 wt% of TiO_2, there was a slightly reduction in the permeate flux. But by using 0.75 wt% of TiO_2, the permeate flux could increase. It is important to mention that the permeate flux using 1 wt% TiO_2 was not acceptable as we observed permeate salinity had increased. At low concentration of TiO_2, the TiO_2 nanoparticles were easy to disperse through the membrane surface and within the substrate. This decreases the probability of the formation of macrovoids, large tear-like and long finger-like pores in the membrane that were more probable at higher TiO_2 concentration, i.e., 0.75 wt%. By further addition of TiO_2 nanoparticle (> 0.75 wt%), significant TiO_2 nanoparticles aggregation could happen which might disrupt the polymer chain packing and also extra free spaces for polymer chain movements [23].

Finally, the effect of ZnO nanoparticle concentration on permeate flux of PSf membranes was studied using ZnO concentrations of 0.25–1 wt% as shown in Fig. 7. It was obvious that the best flux was obtained using 0.5 wt% of ZnO concentration. This may be due to the formation of spongy and small tear like pores in PSf membrane. In contrast, a denser and less free volume structure was obtained in membranes that prepared using 0.75 and 1 wt% of ZnO. This result was in agreement with the previous work on gas separation [24].

3.3. Productivity of VEDCMD compared to other desalination process

Since VEDCMD is not widely practiced and completely different than the normal filtration system, e.g. reverse osmosis (RO), here we drew some advantages of VEDCMD based on this study and a few published studies. Firstly, most of the reported water permeability of state-of-the-art RO for seawater desalination ranged from 18 to 34 L/(m^2 h) [24] which we increased to > 35 L/(m^2 h) in this study. Secondly, another significant advantage of the VEDCMD process is its

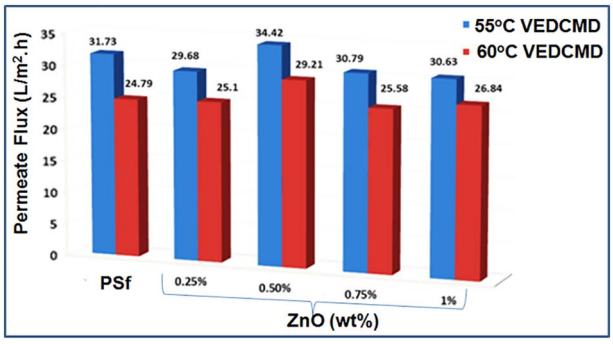

Fig. 7. Effect of ZnO concentration on PSf membrane performance.

minimal effect of feed salt concentration on the permeate flux (Fig. S11). An increased feed salt concentration only marginally decreases the vapor pressure of water and therefore minimally decreases the driving force for mass transfer. On the contrary, increased feed salt concentration significantly decreases the driving force for mass transport and also increases salt passage through the RO membrane. Finally, the primary energy used in RO system is the power required to pump the feed water and is directly related to the feed pressure and flow rate. The high salt concentrations found in seawater require elevated hydrostatic pressures (up to 7000 kPa); the higher the salt concentration, the greater the pressure and pumping power needed to produce a desired permeate flux [34]. Alternatively, VEDCMD can be envisioned to operate using sunlight energy in presence of plasmonic nanomaterials [25] to get warm feed water. Although VEDCMD may require two pumps for operation, one for the feed and one for the permeate; both are typically driven at lower pressures as compared to high pressures of RO-based systems. Therefore, based on these preceding observations, we hypothesized that VEDCMD can be economically more productive for sea water desalination as compared to RO-based filtration system.

4. Conclusions

Firstly, all operational parameters and membrane features were optimized in order to maximize the PSf membranes' performances. For example, DMF was a better solvent than DMA in PSf membrane fabrication in VEDCMD. Increased PSf solvent evaporation time, concentration and membrane thickness could decrease trans-membrane permeate flux. The best coagulation bath temperature varied in the range of 20–30 °C. An increased over these temperatures could lead to permeate flux reduction. There is a positive influence at increase of the feed flow rate, feed temperature, and negative permeate pressure on the permeate flux. On the other hand, there is a negative influence of the feed salt concentration and permeate temperature on the permeate flux of PSf membrane. Different salt types show different PSf membrane selectivity as the permeate flux obeyed the sequence: NaCl > $MgSO_4$ > Na_2SO_4. Secondly, the improvement of PSf membrane was achieved through blending of PSf with carbon-based nanomaterial e.g. MWCNT and inorganic nanoparticles, e.g. mesoporous SiO_2, TiO_2 and ZnO for VEDCMD mediated water desalination. The addition of MWCNT (1), SiO_2 (0.5), TiO_2 (0.75) and ZnO (0.5 wt%) could significantly enhance the permeate flux of PSf membranes.

Appendix A. Supplementary data

Supplementary data to this article can be found online at http://dx.doi.org/10.1016/j.desal.2017.08.020.

References

[1] P. Narong, A. James, Sodium chloride rejection by a UF ceramic membrane in relation to its surface electrical properties, Sep. Purif. Technol. 49 (2006) 122–129.
[2] E.-S.A. Hegazy, B. Nasef, A.M. Dessouki, M.M. Shaker, Ion-containing reverse osmosis membranes obtained by radiation grafting method, Int. J. Radiat. Appl. Instrum. Part C 33 (1989) 13–18.
[3] K.W. Lawson, D.R. Lloyd, Membrane distillation, J. Membr. Sci. 124 (1997) 1–25.
[4] T.Y. Cath, V.D. Adams, A.E. Childress, Vacuum enhanced direct contact membrane distillation, in, Google Patents, 2009.
[5] T.Y. Cath, V.D. Adams, A.E. Childress, Experimental study of desalination using direct contact membrane distillation: a new approach to flux enhancement, J. Membr. Sci. 228 (2004) 5–16.
[6] M. Ali, R. Das, A. Maamor, S.B.A. Hamid, Multifunctional carbon nanotubes (CNTs): a new dimension in environmental remediation, Adv. Mater. Res. 832 (2014) 328–332.
[7] R. Das, M.E. Ali, S.B.A. Hamid, S. Ramakrishna, Z.Z. Chowdhury, Carbon nanotube membranes for water purification: a bright future in water desalination, Desalination 336 (2014) 97–109.
[8] H.A. Shawky, S.-R. Chae, S. Lin, M.R. Wiesner, Synthesis and characterization of a carbon nanotube/polymer nanocomposite membrane for water treatment, Desalination 272 (2011) 46–50.
[9] A. Razmjou, E. Arifin, G. Dong, J. Mansouri, V. Chen, Superhydrophobic modification of TiO_2 nanocomposite PVDF membranes for applications in membrane distillation, J. Membr. Sci. 415 (2012) 850–863.
[10] K. Okiel, A.H.M. El-Aassar, T. Temraz, S. El-Etriby, H.A. Shawky, Performance assessment of synthesized CNT/polypropylene composite membrane distillation for oil field produced water desalination, Desalin. Water Treat. 57 (2016) 10995–11007.
[11] N. Guarrotxena, I. Quijada-Garrido, Optical and swelling stimuli-response of functional hybrid Nanogels: feasible route to achieve tunable smart core@ shell plasmonic@ polymer nanomaterials, Chem. Mater. 28 (2016) 1402–1412.
[12] A. Nechifor, V. Panait, L. Naftanaila, D. Batalu, S. Voicu, Symmetrically polysulfone membranes obtained by solvent evaporation using carbon nanotubes as additives. Synthesis, characterization and applications, Dig. J. Nanomater. Biostruct. 8 (2013) 875–884.
[13] V. Vetrivel, K. Rajendran, V. Kalaiselvi, Synthesis and characterization of pure titanium dioxide nanoparticles by sol-gel method, Int. J. ChemTech Res. 7 (2015) 1090–1097.
[14] W.-H. Lu, K.-D. Li, C.-H. Lu, L.G. Teoh, W.H. Wu, Y.C. Shen, Synthesis and characterization of mesoporous SiO_2–CaO–P_2O_5 bioactive glass by sol–gel process, Mater. Trans. 54 (2013) 791–795.
[15] S. Madaeni, S. Zinadini, V. Vatanpour, Preparation of superhydrophobic nanofiltration membrane by embedding multiwalled carbon nanotube and polydimethylsiloxane in pores of microfiltration membrane, Sep. Purif. Technol. 111 (2013) 98–107.
[16] J. Mo, S.H. Son, J. Jegal, J. Kim, Y.H. Lee, Preparation and characterization of polyamide nanofiltration composite membranes with TiO_2 layers chemically connected to the membrane surface, J. Appl. Polym. Sci. 105 (2007) 1267–1274.
[17] G. Wu, S. Gan, L. Cui, Y. Xu, Preparation and characterization of PES/TiO 2 composite membranes, Appl. Surf. Sci. 254 (2008) 7080–7086.
[18] R.A. Khalkhali, M.B. Keivani, Thermogravimetry analysis of electrochemically synthesized polypyrrole conducting polymer films, Asian J. Chem. 17 (2005) 1483.
[19] R. Das, S.B.A. Hamid, M. Ali, M. Annuar, E.M.B. Samsudin, S. Bagheri, Covalent functionalization schemes for tailoring solubility of multi-walled carbon nanotubes in water and acetone solvents, Sci. Adv. Mater. 7 (2015) 2726–2737.
[20] M. Moniruzzaman, K.I. Winey, Polymer nanocomposites containing carbon nanotubes, Macromolecules 39 (2006) 5194–5205.
[21] R. Das, S.B.A. Hamid, M.E. Ali, A.F. Ismail, M. Annuar, S. Ramakrishna, Multifunctional carbon nanotubes in water treatment: the present, past and future, Desalination 354 (2014) 160–179.
[22] R. Das, M.E. Ali, S.B.A. Hamid, M. Annuar, S. Ramakrishna, Common wet chemical agents for purifying multiwalled carbon nanotubes, J. Nanomater. 2014 (2014) 237.
[23] C.-Y. Liang, P. Uchytil, R. Petrychkovych, Y.-C. Lai, K. Friess, M. Sipek, M.M. Reddy, S.-Y. Suen, A comparison on gas separation between PES (polyethersulfone)/MMT (Na-montmorillonite) and PES/TiO_2 mixed matrix membranes, Sep. Purif. Technol. 92 (2012) 57–63.
[24] P. Moradihamedani, N.A. Ibrahim, W.M.Z.W. Yunus, N.A. Yusof, Study of morphology and gas separation properties of polysulfone/titanium dioxide mixed matrix membranes, Polym. Eng. Sci. 55 (2015) 367–374.
[25] O. Neumann, A.S. Urban, J. Day, S. Lal, P. Nordlander, N.J. Halas, Solar vapor generation enabled by nanoparticles, ACS Nano 7 (2012) 42–49.